Applied Catalysis B: Environmental 201 (2017) 359–369

Contents lists available at ScienceDirect

Applied Catalysis B: Environmental

journal homepage: www.elsevier.com/locate/apcatb

Investigation of metal-exchanged mesoporous Y zeolites for the adsorptive desulfurization of liquid fuels

Kevin X. Lee, Julia A. Valla*

Department of Chemical and Biomolecular Engineering, University of Connecticut, Storrs, CT 06269, USA

ARTICLE INFO

Article history:
Received 27 May 2016
Received in revised form 4 August 2016
Accepted 6 August 2016
Available online 10 August 2016

Keywords:
Mesoporous Y
Sulfur adsorption
Metal-exchanged Y
Metal-exchanged mesoporous Y zeolites

ABSTRACT

Removal of sulfur from transportation fuels using zeolites as sorbents is an attractive desulfurization method, because of its low energy and cost requirements. However, diffusion limitations within the micropore structure of zeolites can reduce their adsorption capacity, especially when refractory sulfur compounds are present in fuels. Moreover, the selective adsorption of sulfur compounds from a mixture of hydrocarbons can be very challenging. The objective of this study was to address the aforementioned challenges of adsorptive desulfurization of fuels using metal-exchanged mesoporous Y zeolites. Mesoporosity was introduced in the Y zeolites by two top-down methods (desilication and surfactant-assisted). Metals, Ce and Cu, were introduced via ion-exchange. The prepared metal-exchanged mesoporous zeolites were characterized and tested in terms of their sulfur adsorption capacity using a fixed-bed column and model fuels. The strength of adsorption was determined using isosteric heat of adsorption calculations. Our results demonstrated that mesoporous Y reduced diffusion limitations and were very effective sorbents for removing sulfur compounds with high kinetic diameter, such as dibenzothiophene (DBT). Metals highly increased the selectivity toward sulfur compounds. According to experimental results, the tendency of thiophenic molecules to adsorb on the zeolites increase in the order of thiophene (TP) < benzothiophene (BT) < DBT. The results of this study revealed that metal-exchanged mesoporous Y zeolites have the potential to display remarkable sulfur removal properties since the mesopores allow access to zeolite active sites while the metal cations improve the selectivity and/or capacity for sulfur compounds.

1. Introduction

Sulfur compounds in transportation fuels, such as diesel and gasoline, are becoming an important global concern, as they pose serious threats to the environment and air quality [1,2]. The Environmental Protection Agency (EPA) regulations regarding air quality policy in the United States, require that the sulfur content in federal gasoline cannot exceed 10 ppmw by January 1st, 2017, while ultra-low sulfur diesel (ULSD) must contain less than 15 ppmw of sulfur [3,4]. Another importance of deep desulfurization is motivated by the extensive use of liquid hydrocarbon fuels for fuel cell applications. Gasoline and diesel are readily available, easily storable and contain high amount of energy density, making them favorable sources of hydrogen gas for fuel cell systems [5–7]. However, the operation of fuel cells is restricted even by present strict sulfur regulations. In fact, fuels used in Solid Oxide Fuel Cell (SOFC) and Proton Exchange Membrane Fuel Cell (PEMFC) should be kept below 5 ppmw and 0.1 ppmw of sulfur, respectively [6,8–10].

Thus, there is a great scientific interest to develop effective deep desulfurization methods to remove sulfur compounds from fuels [11–14]. Concurrently, the recent recession in oil price has driven commercial vehicle sales upwards, which increases the demand for transportation fuels [15–17]. While considerable amount of research has been invested into renewable energy, the energy sector has also focused toward producing more clean fuels derived from oil to meet the rising demand. Conventional hydrodesulfurization (HDS) is currently the most common desulfurization method used in oil refineries. However, to meet the stringent regulations of close to zero sulfur level, very high operating pressure, temperatures and significant hydrogen consumption must be utilized; these severe conditions are accompanied by high cost and the loss of fuel quality [13,18,19]. Furthermore, conventional HDS of diesel fuels is particularly challenging due to difficulty in removing refractory sulfur compounds, such as dibenzothiophene (DBT) and other

* Corresponding author.
E-mail address: ioulia.valla@uconn.edu (J.A. Valla).
URL: http://mailto:ioulia.valla@uconn.edu (J.A. Valla).

http://dx.doi.org/10.1016/j.apcatb.2016.08.018
0926-3373/

substituted DBTs. These conditions altogether make the HDS very expensive and impractical in industrial settings.

To meet the demanding specifications, many desulfurization technologies have been explored either to completely substitute or to compliment the current HDS technology. Some alternative techniques include oxidative desulfurization [20–22], alkylation [23,24], extraction [25,26], biodesulfurization [27,28] and adsorptive desulfurization [29–32]. Among these, sulfur removal via adsorption (adsorptive desulfurization) has been the most promising technique due to the ability to process sulfur-free liquid fuels at ambient conditions. Despite being cost-effective and environment-friendly, the desulfurization performance highly depends on the type of adsorbent. A wide variety of materials have been studied as sorbent materials for sulfur, such as carbon [33,34], oxides [9,35–37], mesoporous materials [38–42], and zeolites [43–49]. The Y zeolite, in particular, has been widely investigated due to the unique faujasite (FAU) pore structure, large surface area, and available surface acidity. The three-dimensional channels, cages and pore diameter of 7.4 Å give the Y zeolite molecular-sieve and shape selective properties, allowing only certain guest species to enter [50]. These properties of Y zeolite make this material one of the most effective zeolites in adsorptive desulfurization. However, the unique microporous nature of the Y zeolites imposes diffusion limitations to refractory sulfur molecules. Additionally the low Si/Al ratio of 2.43 of the Y zeolite results in high Brønsted acid sites (BAS), which play a significant role in sulfur adsorption [51–55].

To overcome the aforementioned limitations, various functionalities, such as mesoporosity and metals, need to be introduced to the zeolite Y. The introduction of mesoporosity allows for more bulkier sulfur compounds, such as dibenzothiophene (DBT) and 4,6-dimethyldibenzothiophene (4,6-DMDBT), to enter the zeolite cages, thus improving accessibility to the active sites. Fu et al. investigated the removal of 4,6-DMDBT through HDS on mesoporous zeolite Y as a support and found that the mesoporosity is favorable for mass transfer and access of aforementioned bulky molecules, consequently increasing the adsorption capacity by 38% compared to the corresponding parent HY zeolite. [56]. The introduction of metal cations can contribute to high selectivity and/or capacity for sulfur. Yang et al. performed pioneering studies on the role of ion-exchanged Y zeolites with transition metals on the desulfurization of fuels [46,57,58]. The group demonstrated that Ag-, Cu-, and Ni-exchanged Y zeolites exhibit high capacities for thiophenic molecule adsorption, among which CuY performs the best by producing 15 mL of thiophene-free model fuel per gram of sorbent. They suggested that the adsorption mechanism proceeds via π-complexation and they found that competitive adsorption becomes a major limitation when other aromatics and foreign species are present in the liquid mixture. Song. et al. determined that CeY has the highest selectivity for removing sulfur from jet fuels due to the strong direct sulfur-metal (S-M) interaction, rather than via π-complexation [59,60]. This has been confirmed by Wang et al. when they demonstrated that CeY is selective to thiophenes compared to olefins in the same hydrocarbon feed [43]. Mesoporous materials with metals have been investigated recently for sulfur adsorption. Yang et al. investigated metal halides supported on mesoporous MCM-41 and SBA-51 for the desulfurization of light jet fuel in a fixed-bed adsorption setup [39]. Oliver et. al studied the adsorptive desulfurization of jet fuel using Ag impregnated MCM-41 and mesoporous silica nanoparticles (MSN), which exhibit adsorption capacities of 32.6 mg S/g and 25.4 mg S/g, respectively [61]. In a more recent study, the group synthesized mesoporous S-impregnated zirconia-silica framework and studied its ability to remove BT, DBT, 4-6-DMDBT and naphthalene in a batch process. The combination of Ag and mesoporous silica substantially increased the adsorption capacity to 39.4 mg S/g [42]. However, all the aforementioned studies have been performed using less acidic, highly siliceous zeolites. Limited studies have been reported so far in investigating the use of mesoporous Y zeolite [62]. Since it has been already demonstrated in the literature that the Y zeolite is one of the best sorbents for the sulfur removal due to their unique acid sites and ion exchange capability, it would be very interesting to investigate the role of mesoporosity in this type of zeolite.

Thus, the objective of this work is to prepare, characterize and test the role of mesoporous, ion-exchanged Y zeolites on the adsorptive removal of sulfur compounds from liquid fuels. Mesoporosity has been created by using two top-down methods. Ce and Cu were ion exchanged in both the parent and the mesoporous Y. The desulfurization tests have been performed in a fixed bed column, using model fuels spiked with thiophene, benzothiophene and dibenzothiophene. Our results demonstrate that there are diffusion limitations for the refractory sulfur compounds, which can be successfully overcome using mesoporous Y zeolites. Furthermore, metal-exchanged mesoporous Y zeolites are very promising in selectively removing the sulfur compounds.

2. Materials and methods

2.1. Preparation of metal-exchanged mesoporous Y zeolites

Fresh NH_4Y zeolite with Si/Al = 2.43 was purchased from Zeolyst International. Mesoporous Y has been prepared using two top-down methods: (a) desilication (DS) and (b) surfactant-assisted (SA) method. Details on the preparation methods can be found in the literature [63–65]. Briefly, desilication has been performed in a 0.05 M NaOH solution, followed by ion-exchange using 0.1 M NH_4NO_3 and calcination at 550 °C for 5.5 h [63]. Surfactant-assisted method has been conducted with acid washing of NH_4Y using 0.58 M of citric acid, base treatment using 0.16 M hexadecyltrimethylammonium bromide (CTAB) and 4.4 M ammonium hydroxide (NH_4OH), followed by calcination at 550 °C for 5.5 h [65]. Ion-exchanged zeolites were prepared using an ion-exchange method with 5 wt% of the desired metal element. Metal precursors $Ce(NO_3)_3{\cdot}6H_2O$ and $Cu(NO_3)_2{\cdot}2.5H_2O$ with at least 99.99% trace metal were purchased from Sigma-Aldrich. To ensure a complete exchange, zeolites and metal precursors were allowed to stir at room temperature for two full days, followed by subsequent washing and drying. The dried materials were then calcined at the same conditions described previously. The final step involved the reduction of metal ions using pure hydrogen gas at 350 °C for 3 h. To prepare metal-exchanged mesoporous zeolites, mesoporous DS and SA Y zeolites were ion-exchanged with the desired metal precursor using the same ion-exchange procedure as the parent Y, followed by calcination and reduction.

2.2. Reagents

To create a controllable environment and for more credible comparison with the literature, reagent grade *n*-octane purchased from Sigma Aldrich was used as a model fuel (solvent). The octane was spiked with pure thiophene (TP), benzothiophene (BT) and dibenzothiophene (DBT), all of which were purchased from Sigma Aldrich. For individual testing, 50 ppmw, 100 ppmw and 150 ppmw of TP, BT and DBT, respectively, were prepared. A model fuel containing all three sulfur compounds was also prepared and tested to represent conventional commercial fuels more closely.

2.3. Material characterization

Crystallinity and microporosity of the materials have been characterized using X-ray diffraction, obtained using a Bruker D8 advanced x-ray diffractometer. Pore structure and surface area were determined using a Micromeritics ASAP 2020 analyzer and

the data were analyzed based on the Brunaeur, Emmert and Teller (BET) method. Brønsted acid sites (BAS) and Lewis acid sites (LAS) in the zeolite as well as metals were qualitatively and quantitatively characterized by pyridine and CO adsorptions, respectively, using a Nicolet 6700 Fourier transform infrared spectrometer (FTIR) equipped with a diffuse reflectance (DRIFT) cell by Harrick. The total amount of metals in the zeolites was determined using an inductively coupled plasma coupled with a mass spectrometer (ICP-MS) following a microwave digestion method [66]. The presence of metal ions and metal oxides on ex-situ calcined and reduced zeolites were also characterized using a Shimadzu UV-26000 UV–vis spectrophotometer.

2.4. Fixed-bed adsorption experiment

To test the desulfurization performance of each adsorbent, a fixed-bed adsorption column was custom made. A 30 cm quartz column with a 3/8" outside diameter (OD) and a built-in frit was used to support the adsorbent. The column was packed with zeolite powders until a bed height of 2.5 cm has been reached, fixing the residence time at approximately 0.1 h. The zeolite weight varied between 0.3–0.5 g depending on the zeolite content (e.g. presence of metals and/or mesoporosity). The metal-modified samples were reduced under H_2 flow at 350 °C for 1 h. Metal-free zeolites such as the Parent Y, surfactant-assisted Y and desilicated Y were activated under N_2 flow at 350 °C for 1 h. The change in color to white after the reduction step confirms that the metal-incorporated zeolites have been activated. Temperature-programmed reduction (TPR) results (Fig. S1) show distinct Cu(I)Y peaks at 250 °C and 350 °C in the supercage and sodalite cage, respectively. A model fuel was fed into the column at a flow rate of 0.05 mL/min and the effluent was collected every 0.5 mL until a saturation point was reached. The sulfur content of the effluents was quantified by a chromatography system equipped with a sulfur chemiluminescence detector (GC-SCD).

2.5. Heat of adsorption by adsorption isotherm

Adsorption isotherms were collected by a batch method. Solutions containing BT or DBT dissolved in octane with concentrations ranging from 100 ppmw to 600 ppmw were prepared. 5 mL of sulfur solution and 50 mg of sorbent were placed inside a flask and allowed to stir for 5 h. The two adsorption temperatures were 20 °C and 50 °C. After adsorption, the solution was washed and the supernatant liquid was collected and analyzed for sulfur content using the GC-SCD.

3. Results

3.1. Characterization results

The retention of the original faujasite crystal structure is important for creating sulfur removal and ion-exchange sites. Fig. 1 shows the XRD results for the parent Y, the mesoporous Y prepared by SA and DS methods, and the Ce and Cu-exchanged Y. Comparing to that of the Y zeolite, the peak intensities for 5% CeY and 5% CuY were reduced due to the presence of foreign entities. Additionally, no peaks of oxides were identified. The mesoporous Y showed a decrease in XRD patterns, where DSY showed lower peak intensity compared to SAY. These reductions in peak intensities were expected, and they suggest that the modifications on the parent material do in fact reduce the crystallinity of the parent Y [67]. Nonetheless, most of the characteristic trends were preserved as shown by the diffraction patterns.

Fig. 2(a) shows the N_2 adsorption/desorption isotherms of all the materials. As expected, the parent Y is very microporous as shown

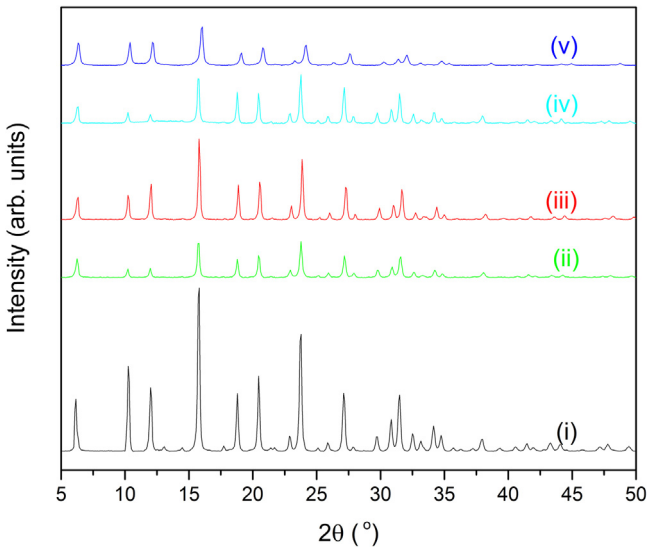

Fig. 1. XRD patterns of parent and modified Y zeolites: (i) Parent Y, (ii) DSY, (iii) SAY, (iv) CuY, (v) CeY.

Table 1
Surface areas and pore volumes of parent and modified Y zeolites.

Material	S_{tot} (m^2/g)	S_{micro} (m^2/g)	S_{meso} (m^2/g)	V_{tot} (cm^3/g)	V_{micro} (cm^3/g)	V_{meso} (cm^3/g)
Parent Y	574	530	43.9	0.282	0.246	0.036
SAY	693	373	319	0.373	0.172	0.201
DSY	646	446	201	0.368	0.206	0.162
CeY	550	500	50.1	0.273	0.232	0.041
CuY	628	394	57.2	0.281	0.229	0.052
CeSAY	648	413	235	0.342	0.190	0.152
CuSAY	637	411	226	0.336	0.190	0.146

by the high nitrogen uptake at low relative pressure. When mesoporosity is introduced, a reduction in microporosity was observed for both the SAY and DSY. The difference between two types of mesoporous materials (SA and DS) becomes clearer on the pore size distribution graph created by the Density Functional Theory (DFT) method, which is presented in Fig. 2(b). The SAY shows a uniform distribution of pores ranging between 20 and 50 Å, whereas the DSY displays a broad range of pores up to about 100 Å. These results are consistent with the literature [64]. Table 1 confirms that the mesopore area and pore volume are increased significantly for the mesoporous materials. The N_2 isotherms for 5% CeY and 5% CuY show a slight decrease in the isotherm plateau due to the presence of foreign entities, which is consistent with the reduction of peaks intensity reported by XRD [68,69]. The metal-exchanged mesoporous zeolites depict a combination of trends, wherein the mesopore area and volume were greatly enhanced and the isotherms were slightly decreased due to the presence of metal ions. Fig. 2 and Table 1 are convincing characteristic results that suggest retention of crystal structure of the modified Y zeolites.

To quantify the acid sites on the sorbent materials, pyridine adsorption experiments were carried out. Pyridine is commonly used as probe molecule for surface acidity detection as the molecule can form pyridium ions with BAS and can bond molecularly to LAS via electron transfer, both of which can be detected using FTIR. Fig. 3 shows the FTIR results obtained from the pyridine adsorption experiment, where the BAS gives vibration peaks at 1543 cm^{-1} and LAS at 1453 cm^{-1}. As expected, the parent Y contains a high amount of BAS due to the high number of framework alumina. The SAY zeolite shows a reduction in BAS/LAS ratio, suggesting a shift from framework to extra-framework alumina due to the introduction of mesoporosity, as presented in Table 2. A more significant shift was

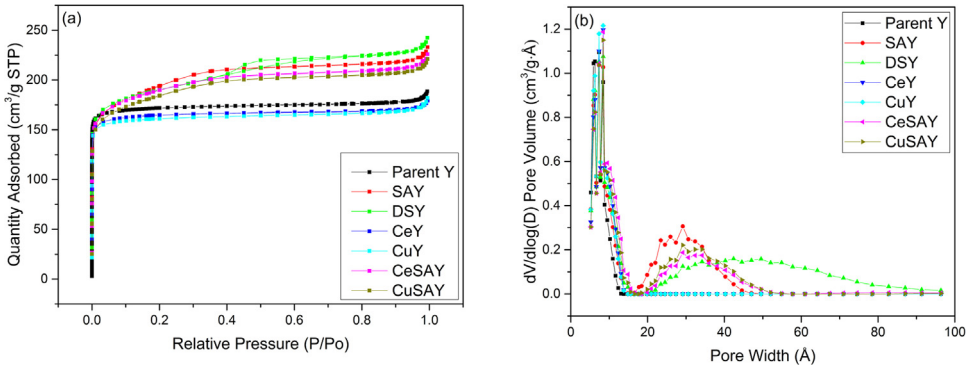

Fig. 2. (a) Nitrogen adsorption-desorption isotherms and (b) DFT pore size distribution of the parent and modified Y zeolites.

Table 2
Brönsted and Lewis acid sites, and metal content in each adsorbent.

Material	Brösted Acidity[a] (μmol/g cat)	Lewis Acidity[a] (μmol/g cat)	Ratio	Ce[b] (wt%)	Cu[b] (wt%)
Parent Y	113.9	30.2	3.77	–	–
SAY	98.2	35.0	2.81	–	–
DSY	56.6	43.9	1.29		
CeY	82.1	20.5	4.00	5.5	–
CuY	43.7	69.3	0.63	–	4.9
CeSAY	–	–	–	5.6	–
CuSAY	–	–	–	–	4.6

[a] Brönsted and Lewis acid sites were calculated using pyridine adsorption.
[b] Ce and Cu metal content were determined using ICP-MS.

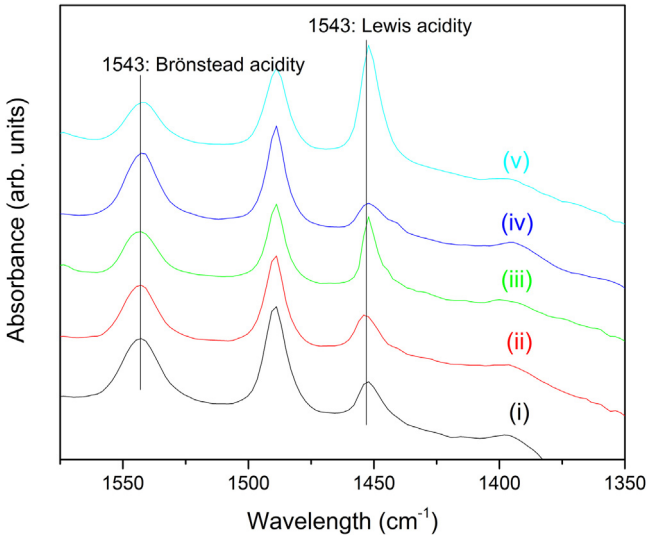

Fig. 3. FTIR spectra of pyridine adsorption on parent and modified Y: (i) Parent Y, (ii) DSY, (iii) SAY, (iv) CuY, (v) CeY.

reported for the DSY zeolite due to the severe desilication procedure used to introduce mesoporosity. An interesting phenomena was observed for the metal-exchanged Y materials. The introduction of Cu to the parent Y increases the LAS, which is accompanied by a decrease in BAS. On the contrary, pyridine adsorption on CeY revealed higher number of BAS compared to LAS. Similar pyridine adsorption results on CeY and CuY have been reported in previous studies [70–72]. The reason for contrasting BAS/LAS ratios between the two metals could be related to the way the metals are distributed, which will be discussed based on the CO adsorption results in the next section. The determination of total amount of metals was carried out using an ICP-MS. The amount of Cu and Ce metals in each Y-type adsorbent is reported in Table 2. The ICP results show that the metal content in each metal-modified material is close to 5 wt%, which validates the ion-exchange procedure and agrees with the theoretical values.

CO is one of the most-used probe molecules for investigating oxidation and coordination states of ions. The kinetic diameter of a CO molecule is 0.376 nm which enables it to easily access the interconnecting channels and pores of the Y zeolite [73,74]. Fig. 4 shows the FTIR spectra of CO adsorption on parent Y and ion-exchanged Y zeolites. The various vibrational peaks correspond to CO interactions with different active sites within the zeolite. Fig. 4(a) illustrates the FTIR spectra of CO adsorbing onto CeY. At low partial pressure of CO, the IR spectrum is relatively flat. As the partial pressure of CO increased, three vibrational peaks at 2170, 2119, and 1636 cm^{-1} emerged, which could be easily desorbed upon evacuation. This finding suggests the absence of CO-to-metal interaction. To confirm this, a spectrum of CO adsorption on parent Y was included in Fig. 4(a) and it was observed to be very similar to that of physisorbed CO on CeY. The broad band on the far right at 1636 cm^{-1} represents the interaction of CO with the aluminosilicate framework [75]. At 80 °C, almost all the physisorbed CO has been desorbed from CeY. Fig. 4(b) shows the FTIR spectra of CO adsorption on CuY zeolite. The main difference with CuY is seen at low partial pressure of CO. Two very stable characteristic peaks at 2144 cm^{-1} and 2158 cm^{-1} correspond to Cu on active sites II and II', respectively, both of which are located on the hexagonal planes of the sodalite cages [73,76,77]. These stable peaks confirmed that CO was chemisorbed on CuY, as opposed to being physisorbed on parent Y and CeY, as shown previously. At elevated CO concentration, new vibrational bands are formed as a result of the decomposition of the initial monocarbonyl species to Cu(I)-CO_2 dicarbonyl species. The bands at 2158 and 2179 cm^{-1} correspond to asymmetrical and symmetrical stretches of dicarbonyl CO on Cu(I) at site II [73,76]. The peak at 2137 cm^{-1} suggests that some monocarbonyl Cu(I)-CO are still present at high CO partial pressure. A higher temperature (ca. 180 °C) was required to remove the strongly bound CO from CuY.

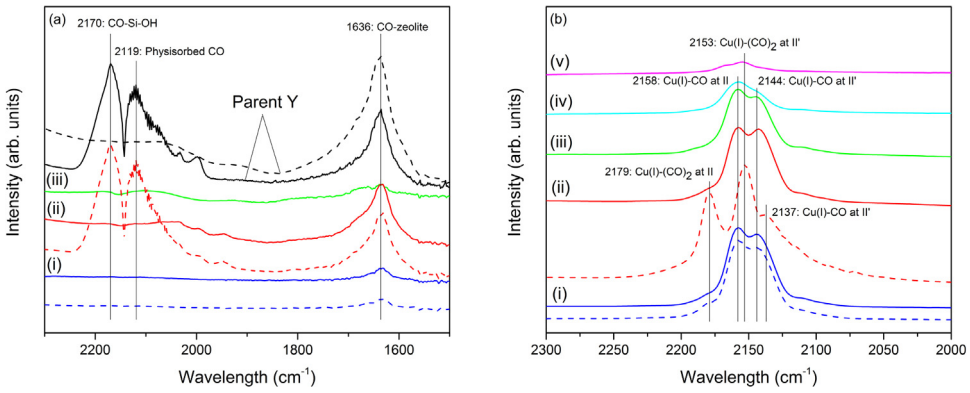

Fig. 4. FTIR spectra of CO adsorption on (a) CeY and (b) CuY at the following conditions: (i) 0.25% CO, (ii) 5% CO, (iii) outgassed at 80 °C, (iv) outgassed at 150 °C, and (v) outgassed at 180 °C. The dotted lines (- - -) represent the spectra after outgassing at room temperature.

The difference in strength of chemisorbed CO on Ce or Cu can be explained by understanding the faujasite structure and its active sites. Metal cations can occupy three main sites in the zeolite framework. Site I and I' are located at the center of the hexagonal prism and inside the sodalite cage, respectively. Site II and II' are located at the faces of the 6 membered ring. A schematic showing the available actives sites is included in Fig. S2. The Y zeolites exhibit sites I, I', II, and II'. Upon ion-exchange, the metal cations occupy only site II. During calcination, the cations migrate toward the hidden sites (eg. sites II', I' and I). Cu cations have shown to favor any coordination sites, while higher charged cations, such as Ce, exhibit greater affinity for type I and I' sites [78–80]. The pores leading to these sites, however, are relatively small and would not permit the access of CO molecules, and hence the absence of chemisorbed-CO vibrational peaks on CeY samples.

The oxidation state at which the metal-modified materials are used during characterization and testing is important for consistency and precision. This is because uncontrolled layers of oxide forming on the metal ions can prevent or weaken the adsorption of thiophenic molecules [9,49]. As previously demonstrated, small amounts of oxides or metal cations favoring the internal sites cannot be detected by XRD or FTIR. One way to confirm the oxidation state of ion-exchanged zeolites is via UV–vis spectroscopy. Fig. 5(a) shows the UV–vis spectroscopy results of Parent Y and CeY. The broad band at 250 nm typically refers to metal oxides, which are exhibited by oxidized CeY (CeY ox). The reduced form of CeY shows four characteristic peaks at 222 nm, 237 nm, 254 nm, and 281 nm. According to the literature, the bands at 222 nm and 281 nm are attributed to the transfer of bond charge from $O \rightarrow Ce^{4+}$, while the bands at 237 nm and 254 nm are assigned to $O \rightarrow Ce^{3+}$ bond charge transfer [81,82]. This confirms that the reduced CeY used in adsorption tests was activated. Fig. 5(b) displays the UV–vis spectrum of Parent Y and CuY. The peak at 212 nm confirms the presence of Cu^{+} metal ions. Unfortunately, due to the rapid oxidation of CuY, the broad band from 600 nm to 1200 nm prevents the characterization of Cu^{2+} on activated CuY and oxidized CuY (CuY ox) [83]. The emergence of oxidation peaks could be eliminated if the activation of zeolites was performed in-situ, but the absence of temperature programmed accessory of UV–vis prevented the study. Nonetheless, both physical appearance and TPR results in Fig. S1 confirmed that the zeolites used for the fixed-bed experiments were indeed activated

3.2. Fixed-bed adsorption results

Fig. 6 shows the breakthrough curves of each of the three different thiophenic compounds on a selection of zeolite materials. Fig. 6(a) shows the adsorption behavior of 50 ppmw of TP on parent Y and CeY. 5 mL/g of sulfur-free model fuel were produced. This finding demonstrates that the incorporation of metals does enhance desulfurization performance. Fig. 6(b) shows the breakthrough curve of 100 ppmw BT in octane. Mesoporous SAY zeolite has also been tested to understand if there are any diffusion limitations during adsorption. However, the breakthrough curve of SAY is very similar to that of the parent, which suggests that diffusion limitations of BT to the active sites of the parent Y zeolite do not exist. An increase in adsorption capacity of about 5 mL/g is observed when CeY or CuY were used as the adsorbent, suggesting that metal incorporation improves the TP and BT uptakes. The same sorbent was used for the desulfurization of DBT, but the breakthrough curve of metal-modified Y zeolites no longer improved the sulfur uptake capacity, as seen in Fig. 6(c). One possible reason is that the sulfur compounds with higher kinetic diameter cannot enter the micropores, thus preventing interactions with the active sites in the sodalite cages. Mesoporous DS and SAY zeolites have been tested and a significant improvement in adsorption capacity was observed as an additional 50 mL/g of sulfur-free was produced. This enhancement suggests that diffusion limitations play a significant role on the adsorption of DBT. The addition of metals to the mesoporous SAY (ie. CeSAY and CuSAY) further increases DBT uptake by about 10 fold, resulting in the production of 125 mL/g of sulfur-free fuel. These results suggest that metal-exchanged mesoporous zeolites enhance both diffusion and selectivity for larger thiophenic compounds.

To evaluate the interaction between the sulfur compounds, 100 ppmw of each sulfur compound was mixed in octane and used as feed. Parent Y, CeSAY and CuSAY were used as adsorbents. Fig. 7(a) shows the breakthrough curve of the simulated liquid fuel on parent Y. The parent Y zeolite produced approximately 15 mL/g of fuel, which could be due to the strong acidity of the material. The adsorption kinetics of each sulfur compound, however, is quite similar, suggesting the absence of selective adsorption. Fig. 7(b) displays the adsorption of sulfur compounds on CeSAY. A significant increase in sulfur capacity was observed, where high BT and DBT capacities of 75 mL/g and 100 mL/g were obtained, respectively. The selectivity of each sulfur compound on CeSAY increases in the order of TP < BT < DBT. The different elution times depend on the interaction of each sulfur compound with Ce metal ions. Among them, DBT exhibits the highest electron density, which contributes to the strongest linkage with Ce [84,85]. The strength in electron density decreases with BT followed by TP, which is consistent with the corresponding breakthrough times. Fig. 7(c) represents the adsorption behavior of model fuel on CuSAY. Similar to CeSAY, the metal-exchanged mesoporous zeolite showed an increase in sulfur capacity compared to the parent Y. The elution times for the different sulfur compounds followed the same order as that of

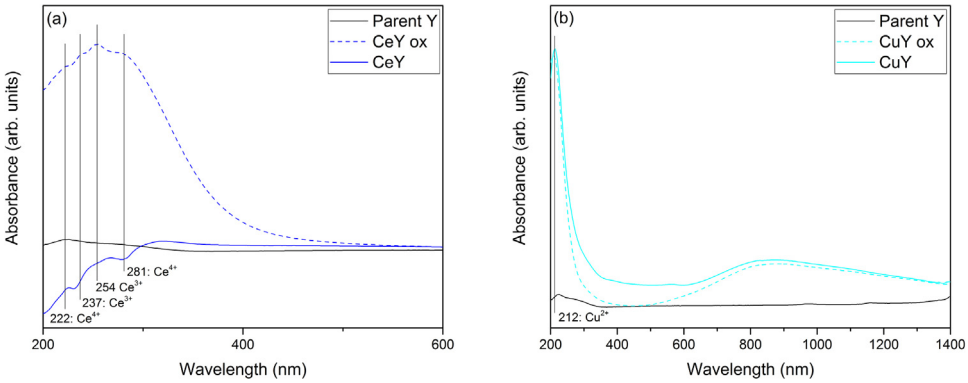

Fig. 5. UV–vis spectra of Parent Y, (a) CeY, and (b) CuY zeolites.

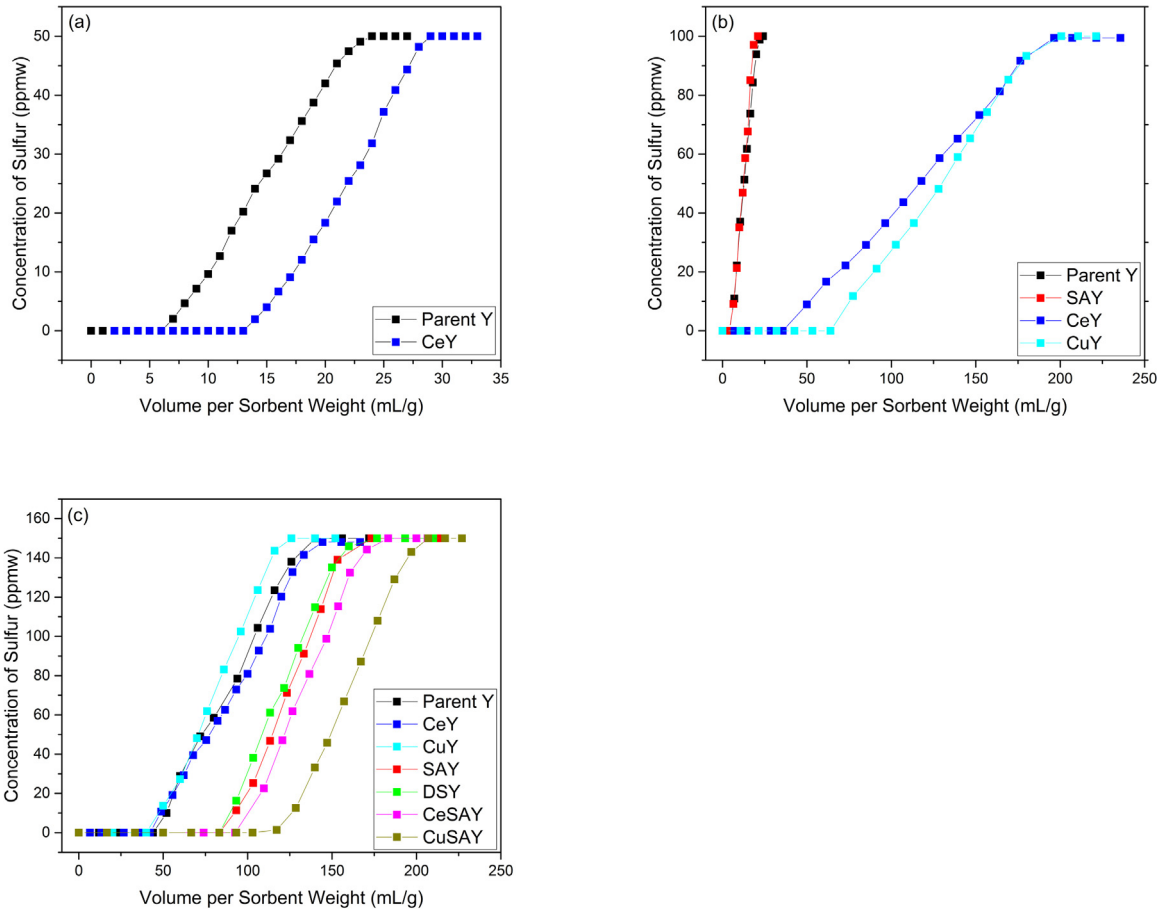

Fig. 6. Breakthrough curves of (a) TP, (b) BT, and (c) DBT on different adsorbents.

CeSAY. However, earlier elution times were observed with CuSAY, in particular for BT and DBT as shown in Fig. 7(c). As discussed earlier, the interactions in which Cu and Ce metals engage with sulfur molecules are different. Transition d-block metals, such as Ni and Cu tend to form π-complexations with neighboring aromatic molecules via back-donation of electron density to the π orbitals [47]. The f-block elements, such as Ce, on the other hand, prefer to selectively form direct σ bonds to nearby molecule [60]. Because DBT possesses the highest electron density among the existing sulfur molecules, the Ce ions will most likely bind stronger to DBT than to BT or TP. This explains the higher elution time of BT and DBT on CeSAY compared to CuSAY, which would otherwise be bound via a relatively weaker π-bond interaction. The breakthrough curve of total sulfur is presented in Fig. 7(d). In conjunction with the individual testing of each compound, metal-exchanged mesoporous zeolites have shown, again, to be the most effective and selective adsorbent for desulfurizing transportation fuels.

3.3. Determination of isosteric heat of adsorption

Isosteric heats of adsorption were calculated to determine the strength of each sorbent when interacting with sulfur molecules. The objective is to correlate the heat of adsorption (ΔH_{ads}) values of each material to the corresponding breakthrough performance. The isosteric heats of adsorption differ from calorimetric experiments, such that the values are derived from the analysis of adsorption

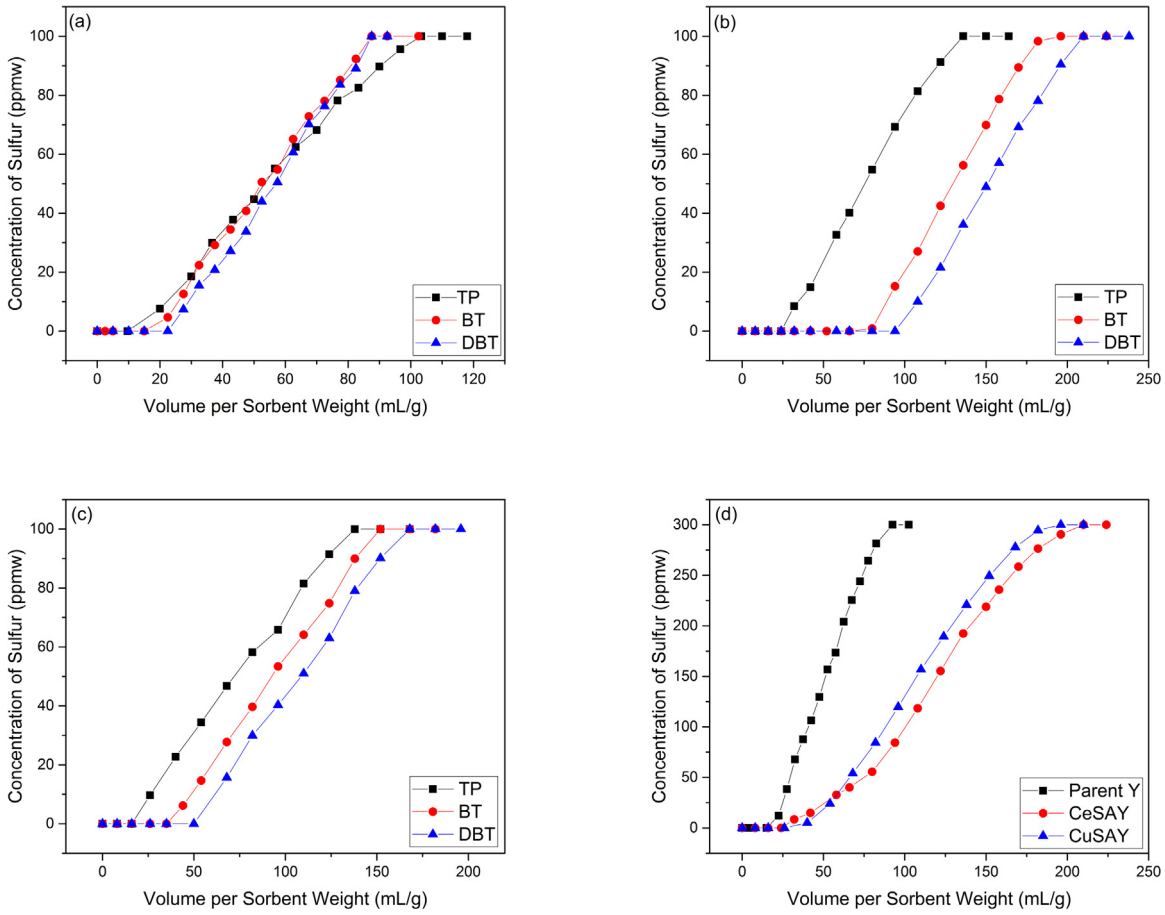

Fig. 7. Breakthrough curves of model fuel on (a) NH_4Y, (b) CeSAY, (c) CuSAY and (d) all sorbents.

isotherms at two varying temperatures [86]. Analogous to vapor-solid adsorption, the enthalpy of adsorption based on the Clausius-Clapeyron equation for liquid-phase adsorption can be written as:

$$\Delta H = -RT^2 \left(\frac{\partial \ln C}{\partial T} \right)_q$$

where C is the equilibrium sulfur concentration (ppmw), T is the adsorption temperature (K), q is the amount of adsorbed sulfur (mmol/g), and R is the universal gas constant. Assuming that the adsorption behavior of sulfur follows the Langmuir isotherm [87], the equilibrium data can be fitted to the following equation:

$$q = \frac{K_L Q_m C}{1 + K_L C}$$

where K_L is the Langmuir constant and Q_m is the maximum amount of adsorbed sulfur. Table 3 shows the adsorption parameters and the corresponding heats of adsorptions. TP is not included in this study because bulky sulfur compounds were the main focus. Moreover, TP has been widely studied in the literature [87,88]. CuY exhibits the highest ΔH_{ads} values as strong adsorption exists between the Cu metal and the sulfur molecule. The calculated ΔH_{ads} values of BT and DBT are also close to those calculated by other groups [73,88] As expected, the adsorption of BT and DBT on the parent Y zeolite is not as strong as on CuY, as also suggested by the breakthrough curves. The similar ΔH_{ads} values of BT and DBT on parent Y shows that the sorbent is not selective and can adsorb equal amount of sulfur compounds, as shown by the breakthrough curve in Fig. 7(a). ΔH_{ads} values of CuSAY and Ultrastable Y were also determined to investigate the influence of pores on sulfur adsorption. The reported ΔH_{ads} values are relatively low, which suggest that the introduction of mesoporosity or the loss of framework alumina could reduce the adsorption strength between the sulfur and the sorbent.

Table 3
Langmuir isotherm parameters and isosteric heats of adsorption for BT and DBT adsorbed on different adsorbents.

Material	Sorbate	T (°C)	K_L (g/mmol)	Q_m (mmol/g)	ΔH_{ads} (−kJ/mol)
Parent Y	BT	20	0.03980	6.740	21.32
		50	0.01380	5.440	
	DBT	20	0.04234	4.524	22.74
		50	0.01812	3.212	
CuY	BT	20	0.01302	0.758	41.94
		50	0.00611	0.375	
	DBT	20	0.03677	2.909	30.46
		50	0.00742	1.911	
CuSAY	DBT	20	0.02994	3.613	15.56
		50	0.01190	3.632	
USY	DBT	20	0.00411	2.469	15.30
		50	0.00248	2.395	

4. Discussion

The goal of the study was to investigate the role of metal-exchanged mesoporous Y zeolites for the adsorptive desulfurization of fuels. Y zeolites are excellent candidates for sulfur adsorption because of their unique pore structure and high density of BAS. Our hypothesis was that the introduction of mesoporosity would allow larger molecules such as DBT to access the internal

active sites of the micropores via σ-bonding or π-complexation. Such modification, however, is inevitably accompanied by the loss of some acid sites. Consequently, the change in active site density will impact the surface chemistry and thermodynamic equilibrium. Meanwhile, metal cations can be introduced into the structure via the ion-exchange method to enhance the selectivity of sulfur compounds. Ion exchange capacity of zeolites is determined by the number of Brønsted acid sites. Reducing the acid sites would result in less ion-exchanged metals in the zeolite, making the zeolite less selective.

Up until now, encouraging results have been reported in literature using mesoporous zeolites [89], or siliceous mesoporous MCM-41 or SBA-15. Metals have also been loaded in MCM-41 and SBA-15 materials [90]. However, to the best of our knowledge, studies on metal-exchanged mesoporous Y zeolites for adsorptive desulfurization are scarce or otherwise limited to batch processes only [29,34,91]. Thus, the novelty of this study comes from the intuition that the combination of both functions of metal-exchanged mesoporous Y zeolites can significantly improve the adsorptive desulfurization in a fixed-bed application. Hence, CeSAY and CuSAY zeolites were prepared to test this hypothesis. Fig. 6(c) confirms the remarkable results from desulfurizing model fuels with CeSAY and CuSAY. Capacity for DBT was significantly increased especially with CuSAY, which reported a 75 mL increase in sulfur-free fuel. To examine the viability of our method, past studies have been compared. Shah et. al investigated the adsorptive performance of Cu-containing SBA-16 which exhibited a capacity up to 40 mL/g for DBT dissolved in *n*-octane [92]. Li et. al performed desulfurization experiments on oxygenated-based activated carbons which effectively removed 60 mL/g of DBT from *n*-octane [93]. Among these materials, metal-exchanged mesoporous Y zeolites have demonstrated predominant desulfurization performance with a high DBT capacity of 125 mL/g. This shows that the proposed metal-exchanged mesoporous zeolites can perform just as effective as other well-distinguished sorbents for desulfurization, if not better.

The strong adsorption capabilities of metal-exchanged mesoporous Y zeolites are also demonstrated in Fig. 7. DBT exhibits relatively higher electron density than other sulfur molecules, which makes it highly favorable for adsorption on the active sites. The presence of DBT causes steric hindrance due to its high kinetic diameter of ~9 Å [94] and inability for other molecules to access the active sites, suggesting that diffusion can be a limiting factor. The mass transfer limitations can be overcome by making the parent Y mesoporous. As pore access becomes possible, the thermodynamic equilibrium constant increases, which results in higher sulfur uptake. For smaller sulfur compounds such as TP and BT, the relatively smaller kinetic diameters allow them to access the supercage freely and subsequently the active sites without any diffusion limitations. The comparable breakthrough slopes of TP, BT and DBT suggest that the role of kinetic rate on sulfur adsorption is inconclusive. Thus, we suggest that the adsorptive desulfurization by metal-exchanged mesoporous Y zeolites is mainly driven by thermodynamics. By eliminating diffusion and selectivity limitations, metal-exchanged mesoporous zeolites show high tendency in adsorbing higher amounts of sulfur, especially the refractory sulfur compounds such as DBT.

Our results indicate that Cu has a higher capacity than that of Ce in the adsorption of single sulfur compound. Analysis of our FTIR results clarifies and distinguishes the difference on the location of Ce and Cu metals. In Fig. 4, chemisorbed CO is absent from the CeY spectrum, whereas strongly-adsorbed CO was observed in the CuY spectrum. CeY occupies very obscure locations such as Site I and I' which are too confined for CO to enter [79,95]. Ce cations favor the migration into the hidden sites, because they can form higher coordination bonds with 6 oxygen ligands [79]. The pores leading to these sites, however, are relatively small and would not permit the access of CO molecules. Hence, the absence of chemisorbed-CO vibrational peaks on CeY samples. Sites II and II' occupied by Cu, on the other hand, are very approachable by CO, as well as for the adsorption of thiophene and other relevant compounds. However, in the mixture of multiple sulfur compounds, Ce cations have shown to be more selective for DBT removal due to strong direct S—M bonds. This could be due to the migration of Ce cations in hidden sites toward the supercage as a result of the tendency to form high energy complexes with thiophenes via the strong σ bond interaction [80]. These results suggest that the affinity of thiophenic molecules to adsorb on the active sites would depend on the type of metal and its location.

It is also interesting that the affinity of each ion-exchanged material to adsorb each sulfur compound follows the same trend. The elution time is held longest for DBT adsorption, followed by BT and TP subsequently, as shown in Fig. 6. To confirm this adsorption trend, a mixture of model fuel containing all three sulfur compounds simultaneously were tested on metal-exchanged mesoporous zeolites. Fig. 7 shows that DBT is most strongly adsorbed compared to BT and T, confirming the aforementioned trend. This leads us to conclude that DBT exhibits the highest electron density among the competing molecules and thus, would form the highest energy bond with the active site. The validation of this conclusion using computational studies will be the objective of our upcoming work.

Heats of adsorption were also measured to determine the nature and bond strength exhibited between thiophenes and zeolites using the isosteric method [87]. In fact, this particular study was directed mainly toward investigating the effects of metals such as Cu on the heat of adsorption. Results showed that ΔH_{ads} is the highest for CuY for both BT and DBT compounds, which is up to twice as much compared to the parent Y. The increase in ΔH_{ads} shows that Cu metals are responsible for stronger sulfur adsorption, which increases the bond strength between the sorbent and the sorbate. This also indicates that the higher adsorption energy is thermodynamically favored, thus increasing the sorbate uptake at equilibrium on CuY. Notice however, a decrease in ΔH_{ads} for DBT adsorbed on the same sorbent, which is consistent with the unchanged breakthrough curves as a result of diffusion limitation. To confirm the hypothesis, the ΔH_{ads} of DBT on CuSAY was measured and the results showed a decrease in energy value. As explained previously, the introduction of mesoporosity may grant access to diffusion into the internal sites, but the trade-off is a reduction of adsorption sites. Nonetheless, the heat of adsorption calculation is a useful tool for comparing binding energies of different aromatics.

The design of metal-exchanged mesoporous Y zeolites explores the balance between the embodiment of active metals and mesopores for adsorptive desulfurization of liquid fuels. For instance, overloading of metals can cause formation of oxides that may block zeolite active sites. Also, mesoporosity should be introduced carefully to avoid uncontrolled desilication of material. Our results have shown that most of the crystal structure and microporosity of modified materials were retained. However, if the materials were recycled and regenerated for further adsorption studies, we would expect some physical change over time depending on the method of regeneration [46,58]. The impact of regeneration on the lifetime of sorbent is an important subject from economic and environmental standpoints, thus will be addressed in our next studies. Overall, good correlation has been demonstrated between theoretical insight and experimental results as shown by the good agreement between breakthrough performance and the predicted ΔH_{ads} of each material.

Finally, it should be pointed out that in this study a linear hydrocarbon – octane – has been used as a model fuel. However, fuels

like gasoline or diesel contain a vast number of other chemical components, such as aromatic hydrocarbons, which might have an inhibiting effect on the adsorption of sulfur compounds [46,70]. The viability and practicality of metal-exchanged mesoporous zeolites in the presence of aromatic hydrocarbons, such as benzene, toluene and naphthalene will be explored in our next studies.

5. Conclusion

Breakthrough measurements of adsorptive desulfurization have been investigated on parent Y, mesoporous Y, metal-exchanged Y and metal-exchanged mesoporous Y zeolites. metal-exchanged mesoporous zeolites, prepared by ion-exchanging mesoporous SAY zeolites with Ce or Cu, exhibit high sulfur adsorptive properties. The experimental results showed that CuSAY zeolite produced 125 mL/g of DBT-free liquid fuel, followed by 100 mL/g by CeSaY. metal-exchanged mesoporous zeolites enhance both accessibility to the active sites and selectivity for thiophenic compounds with high kinetic diameter. This enhancement is driven by the presence of metals which create more active sites to bind with the sulfur either via π-complexation or the direct S-M σ bond. The incorporation of mesoporosity can provide access of bulky sulfur compounds to the active sites. For each material tested, the preference for adsorbing sulfur compounds from octane followed the order of TP < BT < DBT. This trend agreed with the ΔH_{ads} values of each sorbent-sorbate interaction. In a model fuel containing a mixture of all sulfur compounds, CeSAY exhibited the highest sulfur capacity due to strong selective adsorption. This study shows that metal-exchanged mesoporous Y zeolite is a promising candidate for industrial deep desulfurization of transportation fuels. Finding the optimum balance between the pore structure and metals in a metal-exchanged mesoporous zeolite is essential for maximizing capacity and selectivity for sulfur compounds.

Acknowledgement

This work was supported by the American Chemical Society (PRF+ 55900-DN15).

Appendix A. Supplementary data

Supplementary data associated with this article can be found, in the online version, at http://dx.doi.org/10.1016/j.apcatb.2016.08.018.

References

[1] C. Song, X. Ma, New design approaches to ultra-clean diesel fuels by deep desulfurization and deep dearomatization, Appl. Catal. B Environ. 41 (2003) 207–238, http://dx.doi.org/10.1016/S0926-3373(02)00212-6.
[2] A. Stanislaus, A. Marafi, M.S. Rana, Recent advances in the science and technology of ultra low sulfur diesel (ULSD) production, Catal. Today 153 (2010) 1–68, http://dx.doi.org/10.1016/j.cattod.2010.05.011.
[3] X. Ma, K. Sakanishi, I. Mochida, Hydrodesulfurization reactivities of various sulfur compounds in diesel fuel, Ind. Eng. Chem. Res. 33 (1994) 218–222, http://dx.doi.org/10.1021/ie00026a007.
[4] Office of Transportation and Air Quality, EPA sets Tier 3 motor vehicle emissions and fuel standards, United States Environ. Prot. Agency, 2014. https://www3.epa.gov/otaq/documents/tier3/420f14009.pdf (accessed 02.03.16).
[5] J.H. Kim, X. Ma, A. Zhou, C. Song, Ultra-deep desulfurization and denitrogenation of diesel fuel by selective adsorption over three different adsorbents: a study on adsorptive selectivity and mechanism, Catal. Today 111 (2006) 74–83, http://dx.doi.org/10.1016/j.cattod.2005.10.017.
[6] V.M. Bhandari, C.H. Ko, J.G. Park, S.S. Han, S.H. Cho, J.N. Kim, Desulfurization of diesel using ion-exchanged zeolites, Chem. Eng. Sci. 61 (2006) 2599–2608, http://dx.doi.org/10.1016/j.ces.2005.11.015.
[7] J.A.Z. Pieterse, S. Van Eijk, H.A.J. Van Dijk, R.W. Van Den Brink, On the potential of absorption and reactive adsorption for desulfurization of ultra low-sulfur commercial diesel in the liquid phase in the presence of fuel additive and bio-diesel, Fuel Process. Technol. 92 (2011) 616–623, http://dx.doi.org/10.1016/j.fuproc.2010.11.019.
[8] J.C. Zhang, L.F. Song, J.Y. Hu, S.L. Ong, W.J. Ng, L.Y. Lee, et al., Investigation on gasoline deep desulfurization for fuel cell applications, Energy Convers. Manag. 46 (2005) 1–9, http://dx.doi.org/10.1016/j.enconman.2004.02.005.
[9] M. Xue, R. Chitrakar, K. Sakane, T. Hirotsu, K. Ooi, Y. Yoshimura, et al., Preparation of cerium-loaded Y-zeolites for removal of organic sulfur compounds from hydrodesulfurizated gasoline and diesel oil, J. Colloid Interface Sci. 298 (2006) 535–542, http://dx.doi.org/10.1016/j.jcis.2005.12.051.
[10] F.A. Duarte, P. de, A. Mello, C.A. Bizzi, M.A.G. Nunes, E.M. Moreira, M.S. Alencar, et al., Sulfur removal from hydrotreated petroleum fractions using ultrasound-assisted oxidative desulfurization process, Fuel 90 (2011) 2158–2164, http://dx.doi.org/10.1016/j.fuel.2011.01.030.
[11] M. Breysse, G. Djega-Mariadassou, S. Pessayre, C. Geantet, M. Vrinat, G. Pérot, et al., Deep desulfurization: reactions, catalysts and technological challenges, Catal. Today 84 (2003) 129–138, http://dx.doi.org/10.1016/S0920-5861(03)00266-9.
[12] H. Topsøe, Developments in operando studies and in situ characterization of heterogeneous catalysts, J. Catal. 216 (2003) 155–164, http://dx.doi.org/10.1016/S0021-9517(02)00133-1.
[13] C. Song, An overview of new approaches to deep desulfurization for ultra-clean gasoline, diesel fuel and jet fuel, Catal. Today 86 (2003) 211–263, http://dx.doi.org/10.1016/S0920-5861(03)00412-7.
[14] I.V. Babich, J.A. Moulijn, Science and technology of novel processes for deep desulfurization of oil refinery streams: a review, Fuel 82 (2003) 607–631, http://dx.doi.org/10.1016/S0016-2361(02)00324-1.
[15] T. Bowler, Falling oil prices: who are the winners and losers? BBC News (2015), http://www.bbc.com/news/business-29643612 (accessed 02.03.16).
[16] C. Krauss, Oil prices what's behind the drop? Simple economics, New York Times (2016), http://www.nytimes.com/interactive/2016/business/energy-environment/oil-prices.html (accessed 02.03.16).
[17] Q. Wang, R. Li, Impact of cheaper oil on economic system and climate change: a SWOT analysis, Renew. Sustain. Energy Rev. 54 (2016) 925–931, http://dx.doi.org/10.1016/j.rser.2015.10.087.
[18] Y. Wang, J. Latz, R. Dahl, J. Pasel, R. Peters, Liquid phase desulfurization of jet fuel by a combined pervaporation and adsorption process, Fuel Process. Technol. 90 (2009) 458–464, http://dx.doi.org/10.1016/j.fuproc.2008.11.008.
[19] Y. Wang, J. Geder, J.M. Schubert, R. Dahl, J. Pasel, R. Peters, Optimization of adsorptive desulfurization process of jet fuels for application in fuel cell systems, Fuel Process. Technol. 95 (2012) 144–153, http://dx.doi.org/10.1016/j.fuproc.2011.11.011.
[20] A. Chica, A. Corma, M. Domine, Catalytic oxidative desulfurization (ODS) of diesel fuel on a continuous fixed-bed reactor, J. Catal. 242 (2006) 299–308, http://dx.doi.org/10.1016/j.jcat.2006.06.013.
[21] M.T. Timko, E. Schmois, P. Patwardhan, Y. Kida, C.A. Class, W.H. Green, et al., Response of different types of sulfur compounds to oxidative desulfurization of jet fuel, Energy Fuels 28 (2014) 2977–2983, http://dx.doi.org/10.1021/ef500216p.
[22] X. Wu, Y. Bai, Y. Tian, X. Meng, L. Shi, Gasoline desulfurization by catalytic alkylation over methanesulfonic acid, Bull. Korean Chem. Soc. 34 (2013) 3055–3058, http://dx.doi.org/10.5012/bkcs.2013.34.10.3055.
[23] X.D. Zheng, H.J. Dong, X. Wang, L. Shi, Study on olefin alkylation of thiophenic sulfur in FCC gasoline using La2O3-modified HY zeolite, Catal. Lett. 127 (2009) 70–74, http://dx.doi.org/10.1007/s10562-008-9625-z.
[24] X. Jiang, Y. Nie, C. Li, Z. Wang, Imidazolium-based alkylphosphate ionic liquids—a potential solvent for extractive desulfurization of fuel, Fuel 87 (2008) 79–84, http://dx.doi.org/10.1016/j.fuel.2007.03.045.
[25] F. Li, C. Kou, Z. Sun, Y. Hao, R. Liu, D. Zhao, Deep extractive and oxidative desulfurization of dibenzothiophene with C5H9NO·SnCl2 coordinated ionic liquid, J. Hazard. Mater. 205–206 (2012) 164–170, http://dx.doi.org/10.1016/j.jhazmat.2011.12.054.
[26] S. Zhang, Q. Zhang, Z.C. Zhang, Extractive desulfurization and denitrogenation of fuels using ionic liquids, Ind. Eng. Chem. Res. 43 (2004) 614–622, http://dx.doi.org/10.1021/ie030561+.
[27] A.B. Martin, A. Alcon, V.E. Santos, F. Garcia-Ochoa, Production of a Rhodococcus erythropolis IGTS8 biocatalyst for DBT biodesulfurization: influence of operational conditions, Energy Fuels 19 (2005) 775–782, http://dx.doi.org/10.1021/ef0400417.
[28] F. Davoodi-Dehaghani, M. Vosoughi, A.A. Ziaee, Biodesulfurization of dibenzothiophene by a newly isolated Rhodococcus erythropolis strain, Bioresour. Technol. 101 (2010) 1102–1105, http://dx.doi.org/10.1016/j.biortech.2009.08.058.
[29] J. Wang, F. Xu, W.J. Xie, Z.J. Mei, Q.Z. Zhang, J. Cai, et al., The enhanced adsorption of dibenzothiophene onto cerium/nickel-exchanged zeolite Y, J. Hazard. Mater. 163 (2009) 538–543, http://dx.doi.org/10.1016/j.jhazmat.2008.07.027.
[30] C. Meng, Y. Fang, L. Jin, H. Hu, Deep desulfurization of model gasoline by selective adsorption on Ag+/Al-MSU-S, Catal. Today 149 (2010) 138–142, http://dx.doi.org/10.1016/j.cattod.2009.02.038.
[31] A. Samadi-Maybodi, M. Teymouri, A. Vahid, A. Miranbeigi, In situ incorporation of nickel nanoparticles into the mesopores of MCM-41 by manipulation of solvent-solute interaction and its activity toward adsorptive desulfurization of gas oil, J. Hazard. Mater. 192 (2011) 1667–1674, http://dx.doi.org/10.1016/j.jhazmat.2011.06.089.

[32] Y. Wang, R.T. Yang, Desulfurization of liquid fuels by adsorption on carbon-based sorbents and ultrasound-assisted sorbent regeneration, Langmuir 23 (2007) 3825–3831, http://dx.doi.org/10.1021/la063364z.
[33] M.T. Timko, J.A. Wang, J. Burgess, P. Kracke, L. Gonzalez, C. Jaye, et al., Roles of surface chemistry and structural defects of activated carbons in the oxidative desulfurization of benzothiophenes, Fuel 163 (2016) 223–231, http://dx.doi.org/10.1016/j.fuel.2015.09.075.
[34] Y. Yang, H. Lu, P. Ying, Z. Jiang, C. Li, Selective dibenzothiophene adsorption on modified activated carbons, Carbon N. Y. 45 (2007) 3042–3044, http://dx.doi.org/10.1016/j.carbon.2007.10.016.
[35] L. Huang, Z. Qin, G. Wang, M. Du, H. Ge, X. Li, et al., A detailed study on the negative effect of residual sodium on the performance of Ni/ZnO adsorbent for diesel fuel desulfurization, Ind. Eng. Chem. Res. 49 (2010) 4670–4675, http://dx.doi.org/10.1021/ie100293h.
[36] S. Watanabe, X. Ma, C. Song, Selective sulfur removal from liquid hydrocarbons over regenerable CeO2-TiO2 adsorbents for fuel cell applications, ACS Div. Fuel Chem. Prepr. 49 (2004) 511–513.
[37] M. Xue, R. Chitrakar, K. Sakane, T. Hirotsu, K. Ooi, Y. Yoshimura, et al., Selective adsorption of thiophene and 1-benzothiophene on metal-ion-exchanged zeolites in organic medium, J. Colloid Interface Sci. 285 (2005) 487–492, http://dx.doi.org/10.1016/j.jcis.2004.12.031.
[38] W. Li, H. Tang, T. Zhang, Q. Li, J. Xing, H. Liu, Ultra-deep desulfurization adsorbents for hydrotreated diesel with magnetic mesoporous aluminosilicates, AIChE J. 56 (2009), http://dx.doi.org/10.1002/aic.12070.
[39] Y. Wang, R.T. Yang, J.M. Heinzel, Desulfurization of jet fuel by π-complexation adsorption with metal halides supported on MCM-41 and SBA-15 mesoporous materials, Chem. Eng. Sci. 63 (2008) 356–365, http://dx.doi.org/10.1016/j.ces.2007.09.002.
[40] B.S. Liu, D.F. Xu, J.X. Chu, W. Liu, C.T. Au, Deep desulfurization by the adsorption process of fluidized catalytic cracking (FCC) diesel over mesoporous Al-MCM-41 materials, Energy Fuels 21 (2007) 250–255, http://dx.doi.org/10.1021/ef060249n.
[41] S.G. McKinley, R.J. Angelici, Deep desulfurization by selective adsorption of dibenzothiophenes on Ag+/SBA-15 and Ag+/SiO2, Chem. Commun. (Camb.) (2003) 2620–2621, http://dx.doi.org/10.1039/b309249f.
[42] J.M. Palomino, D.T. Tran, A.R. Kareh, C.A. Miller, J.M.V. Gardner, H. Dong, et al., Zirconia-silica based mesoporous desulfurization adsorbents, J. Power Sour. 278 (2015) 141–148, http://dx.doi.org/10.1016/j.jpowsour.2014.12.043.
[43] H. Wang, L. Song, H. Jiang, J. Xu, L. Jin, X. Zhang, et al., Effects of olefin on adsorptive desulfurization of gasoline over Ce(IV)Y zeolites, Fuel Process. Technol. 90 (2009) 835–838, http://dx.doi.org/10.1016/j.fuproc.2009.03.004.
[44] F. Tian, W. Wu, Z. Jiang, C. Liang, Y. Yang, P. Ying, et al., The study of thiophene adsorption onto La(III)-exchanged zeolite NaY by FT-IR spectroscopy, J. Colloid Interface Sci. 301 (2006) 395–401, http://dx.doi.org/10.1016/j.jcis.2006.05.017.
[45] A.J. Hernández-Maldonado, F.H. Yang, G. Qi, R.T. Yang, Desulfurization of transportation fuels by π-complexation sorbents: Cu(I)-, Ni(II)-, and Zn(II)-zeolites, Appl. Catal. B Environ. 56 (2005) 111–126, http://dx.doi.org/10.1016/j.apcatb.2004.06.023.
[46] A.J. Hernández-Maldonado, R.T. Yang, Desulfurization of liquid fuels by adsorption via π complexation with Cu(I)-Y and Ag-Y zeolites, Ind. Eng. Chem. Res. 42 (2003) 123–129, http://dx.doi.org/10.1021/ie020728j.
[47] R.T. Yang, A.J. Hernández-Maldonado, F.H. Yang, Desulfurization of transportation fuels with zeolites under ambient conditions, Science 301 (2003) 79–81, http://dx.doi.org/10.1126/science.1085088.
[48] S. Velu, X. Ma, C. Song, Selective adsorption for removing sulfur from jet fuel over zeolite-based adsorbents, Ind. Eng. Chem. Res. 42 (2003) 5293–5304, http://dx.doi.org/10.1021/ie020995p.
[49] S. Velu, C. Song, M.H. Engelhard, Y.H. Chin, Adsorptive removal of organic sulfur compounds from jet fuel over K-exchanged NiY zeolites prepared by impregnation and ion exchange, Ind. Eng. Chem. Res. 44 (2005) 5740–5749, http://dx.doi.org/10.1021/ie0488492.
[50] D.P. Serrano, J. Aguado, G. Morales, J.M. Rodríguez, A. Peral, M. Thommes, et al., Molecular and meso- and macroscopic properties of hierarchical nanocrystalline ZSM-5 zeolite prepared by seed silanization, Chem. Mater. 21 (2009) 641–654, http://dx.doi.org/10.1021/cm801951a.
[51] J. Liao, W. Bao, Y. Chen, Y. Zhang, L. Chang, The adsorptive removal of thiophene from benzene over ZSM-5 zeolite, Energy Sour. Part A Recover. Util. Environ. Eff. 34 (2012) 618–625, http://dx.doi.org/10.1080/15567036.2010.549916.
[52] S. Nair, B.J. Tatarchuk, Characteristics of sulfur removal by silver-titania adsorbents at ambient conditions, Adsorption 17 (2011) 663–673, http://dx.doi.org/10.1007/s10450-011-9362-2.
[53] S.E. Khalafalla, L.A. Haas, Active sites for catalytic reduction of SO2 with CO on alumina, J. Catal. 24 (1972) 115–120, http://dx.doi.org/10.1016/0021-9517(72)90015-2.
[54] S. Nair, A.H.M. Shahadat Hussain, B.J. Tatarchuk, The role of surface acidity in adsorption of aromatic sulfur heterocycles from fuels, Fuel 105 (2013) 695–704, http://dx.doi.org/10.1016/j.fuel.2012.10.005.
[55] L. Duan, X. Gao, X. Meng, H. Zhang, Q. Wang, Y. Qin, et al., Adsorption, Co-adsorption, and reactions of sulfur compounds, aromatics, olefins over Ce-exchanged y zeolite, J. Phys. Chem. C. 116 (2012) 25748–25756, http://dx.doi.org/10.1021/jp303040m.
[56] W. Fu, L. Zhang, T. Tang, Q. Ke, S. Wang, J. Hu, et al., Extraordinarily high activity in the hydrodesulfurization of 4,6-dimethyldibenzothiophene over Pd supported on mesoporous zeolite Y, J. Am. Chem. Soc. 133 (2011) 15346–15349, http://dx.doi.org/10.1021/ja2072719.
[57] A.J. Hernández-Maldonado, R.T. Yang, Desulfurization of diesel fuels by adsorption via π-complexation with vapor-phase exchanged Cu(I)-Y zeolites, J. Am. Chem. Soc. 126 (2004) 992–993, http://dx.doi.org/10.1021/ja039304m.
[58] A.J. Hernández-Maldonado, R.T. Yang, Desulfurization of diesel fuels via π-complexation with nickel(II)-exchanged X- and Y-zeolites, Ind. Eng. Chem. Res. 43 (2004) 1081–1089, http://dx.doi.org/10.1021/Ie034206v.
[59] S. Velu, X. Ma, C. Song, Zeolite-based adsorbents for desulfurization of jet fuel by selective adsorption, ACS Div. Fuel Chem. Prepr. 47 (2002) 447–448.
[60] X. Ma, S. Velu, J.H. Kim, C. Song, Deep desulfurization of gasoline by selective adsorption over solid adsorbents and impact of analytical methods on ppm-level sulfur quantification for fuel cell applications, Appl. Catal. B Environ. 56 (2005) 137–147, http://dx.doi.org/10.1016/j.apcatb.2004.08.013.
[61] J.M. Palomino, D.T. Tran, J.L. Hauser, H. Dong, S.R.J. Oliver, Mesoporous silica nanoparticles for high capacity adsorptive desulfurization, J. Mater. Chem. A 2 (2014) 14890–14895, http://dx.doi.org/10.1039/C4TA02570A.
[62] F. Tian, Q. Shen, Z. Fu, Y. Wu, C. Jia, Enhanced adsorption desulfurization performance over hierarchically structured zeolite Y, Fuel Process. Technol. 128 (2014) 176–182, http://dx.doi.org/10.1016/j.fuproc.2014.07.018.
[63] D. Verboekend, J. Pérez-Ramírez, Design of hierarchical zeolite catalysts by desilication, Catal. Sci. Technol. 1 (2011) 879, http://dx.doi.org/10.1039/c1cy00150g.
[64] K. Li, J. Valla, J. Garcia-Martinez, Realizing the commercial potential of hierarchical zeolites: new opportunities in catalytic cracking, ChemCatChem 6 (2014) 46–66, http://dx.doi.org/10.1002/cctc.201300345.
[65] J. García-Martínez, M. Johnson, J. Valla, K. Li, J.Y. Ying, Mesostructured zeolite Y—high hydrothermal stability and superior FCC catalytic performance, Catal. Sci. Technol. 2 (2012) 987, http://dx.doi.org/10.1039/c2cy00309k.
[66] F. Subhan, B.S. Liu, Y. Zhang, X.G. Li, High desulfurization characteristic of lanthanum loaded mesoporous MCM-41 sorbents for diesel fuel, Fuel Process. Technol. 97 (2012) 71–78, http://dx.doi.org/10.1016/j.fuproc.2012.01.016.
[67] S. Nuntang, P. Prasassarakich, C. Ngamcharussrivichai, Comparative study on adsorptive removal of thiophenic sulfurs over Y and USY zeolites, Ind. Eng. Chem. Res. 47 (2008) 7405–7413, http://dx.doi.org/10.1021/ie701785s.
[68] Y. Shi, W. Zhang, H. Zhang, F. Tian, C. Jia, Y. Chen, Effect of cyclohexene on thiophene adsorption over NaY and LaNaY zeolites, Fuel Process. Technol. 110 (2013) 24–32, http://dx.doi.org/10.1016/j.fuproc.2013.01.008.
[69] J. Zhang, G. Qiu, L. Fan, X. Meng, Q. Cai, Y. Wang, Enhanced sulfur capacity of durable and regenerable mesoporous sorbents for the deep desulfurization of diesel, Fuel 153 (2015) 578–584, http://dx.doi.org/10.1016/j.fuel.2015.03.056.
[70] H. Song, H. Song, X. Wan, M. Dai, J. Zhang, F. Li, Deep desulfurization of model gasoline by selective adsorption over Cu-Ce bimetal ion-exchanged y zeolite, Fuel Process. Technol. 116 (2013) 52–62, http://dx.doi.org/10.1016/j.fuproc.2013.04.017.
[71] J. Li, P. Zeng, L. Zhao, S. Ren, Q. Guo, H. Zhao, et al., Tuning of acidity in CeY catalytic cracking catalysts by controlling the migration of Ce in the ion exchange step through valence changes, J. Catal. 329 (2015) 441–448, http://dx.doi.org/10.1016/j.jcat.2015.06.012.
[72] Y. Shi, X. Yang, F. Tian, C. Jia, Y. Chen, Effects of toluene on thiophene adsorption over NaY and Ce(IV)Y zeolites, J. Nat. Gas Chem. 21 (2012) 421–425, http://dx.doi.org/10.1016/S1003-9953(11)60385-X.
[73] M. Jiang, F.T.T. Ng, Adsorption of benzothiophene on Y zeolites investigated by infrared spectroscopy and flow calorimetry, Catal. Today 116 (2006) 530–536, http://dx.doi.org/10.1016/j.cattod.2006.06.034.
[74] O. Cairon, A. Loustaunau, Adsorption of CO on NaY faujasite: a revisited FT-IR study, J. Phys. Chem. C 112 (2008) 18493–18501, http://dx.doi.org/10.1021/jp8002382.
[75] V. Rakić, V. Dondur, R. Hercigonja, FTIR study of carbon monoxide adsorption on ion-exchanged X, Y and mordenite type zeolites, J. Serbian Chem. Soc. 68 (2003) 409–416, http://dx.doi.org/10.2298/JSC0305409R.
[76] V.Y. Borovkov, M. Jiang, Y. Fu, Investigation of copper carbonyl species formed upon CO adsorption on copper-exchanged zeolites by diffuse reflectance FTIR, J. Phys. Chem. B 103 (1999) 5010–5019, http://dx.doi.org/10.1021/jp984727+.
[77] V.M. Rakić, R.V. Hercigonja, V.T. Dondur, CO interaction with zeolites studied by TPD and FTIR: transition-metal ion-exchanged FAU-type zeolites, Microporous Mesoporous Mat. 27 (1999) 27–39, http://dx.doi.org/10.1016/S1387-1811(98)00224-8.
[78] G. Turnes Palomino, S. Bordiga, A. Zecchina, G.L. Marra, C. Lamberti, XRD, XAS, and IR characterization of copper-exchanged Y zeolite, J. Phys. Chem. B 104 (2000) 8641–8651, http://dx.doi.org/10.1021/jp000584r.
[79] T.A. Egerton, F.S. Stone, Adsorption of carbon monoxide by zeolite Y exchanged with different cations, J. Chem. Soc. Faraday Trans. 1 Phys. Chem. Condens. Phases 69 (1973) 22, http://dx.doi.org/10.1039/f19736900022.
[80] J.F. Tempère, F. Bozon-Verduraz, D. Delafosse, A kinetic study of the oxidation of cerium ions in an X zeolite, Mater. Res. Bull. 12 (1977) 871–879, http://dx.doi.org/10.1016/0025-5408(77)90098-8.
[81] A. Bensalem, J.C. Muller, F. Bozon-Verduraz, Faraday communications. From bulk CeO 2 to supported cerium–oxygen clusters: a diffuse reflectance approach, J. Chem. Soc. Faraday Trans. 88 (1992) 153–154, http://dx.doi.org/10.1039/FT9928800153.
[82] M.N. Timofeeva, S.H. Jhung, Y.K. Hwang, D.K. Kim, V.N. Panchenko, M.S. Mel'gunov, et al., Ce-silica mesoporous SBA-15-type materials for oxidative catalysis: synthesis, characterization, and catalytic application, Appl. Catal. A—Gen. 317 (2007) 1–10, http://dx.doi.org/10.1016/j.apcata.2006.07.014.

[83] J. Texter, D.H. Strome, R.G. Herman, K. Klier, Chemical and spectroscopic properties of copper containing zeolites, J. Phys. Chem. 81 (1977) 333–338, http://dx.doi.org/10.1021/j100519a011.
[84] Y. Xia, Y. Li, Y. Gu, T. Jin, Q. Yang, J. Hu, et al., Adsorption desulfurization by hierarchical porous organic polymer of poly-methylbenzene with metal impregnation, Fuel 170 (2016) 100–106, http://dx.doi.org/10.1016/j.fuel.2015.12.047.
[85] H. Song, X. Cui, H. Song, H. Gao, F. Li, Characteristic and adsorption desulfurization performance of Ag–Ce bimetal ion-exchanged Y zeolite, Ind. Eng. Chem. Res. 53 (2014) 14552–14557, http://dx.doi.org/10.1021/ie404362f.
[86] S. Builes, S.I. Sandler, R. Xiong, Isosteric heats of gas and liquid adsorption, Langmuir 29 (2013) 10416–10422, http://dx.doi.org/10.1021/la401035p.
[87] L. Ma, R.T. Yang, Selective adsorption of sulfur compounds: isotherms, heats, and relationship between adsorption from vapor and liquid solution, Ind. Eng. Chem. Res. 46 (2007) 2760–2768, http://dx.doi.org/10.1021/ie0700516.
[88] M. Liping, R.T. Yang, Heats of adsorption from liquid solutions and from pure vapor phase: adsorption of thiophenic compounds on NaY and 13X zeolites, Ind. Eng. Chem. Res. 46 (2007) 4874–4882, http://dx.doi.org/10.1021/ie070336i.
[89] F. Tian, X. Yang, Y. Shi, C. Jia, Y. Chen, Adsorptive desulfurization over hierarchical beta zeolite by alkaline treatment, J. Nat. Gas Chem. 21 (2012) 647–652, http://dx.doi.org/10.1016/S1003-9953(11)60414-3.
[90] H. Chen, Y. Wang, F.H. Yang, R.T. Yang, Desulfurization of high-sulfur jet fuel by mesoporous π-complexation adsorbents, Chem. Eng. Sci. 64 (2009) 5240–5246, http://dx.doi.org/10.1016/j.ces.2009.08.031.
[91] J. Jiang, F.T.T. Ng, Production of low sulfur diesel fuel via adsorption: an equilibrium and kinetic study on the adsorption of dibenzothiophene onto NaY zeolite, Adsorption 16 (2010) 549–558, http://dx.doi.org/10.1007/s10450-010-9259-5.
[92] A.T. Shah, B. Li, Z.E.A. Abdalla, Direct synthesis of Cu-SBA-16 by internal pH-modification method and its performance for adsorption of dibenzothiophene, Microporous Mesoporous Mat. 130 (2010) 248–254, http://dx.doi.org/10.1016/j.micromeso.2009.11.017.
[93] W. Zhang, H. Liu, Q. Xia, Z. Li, Enhancement of dibenzothiophene adsorption on activated carbons by surface modification using low temperature oxygen plasma, Chem. Eng. J. 209 (2012) 597–600, http://dx.doi.org/10.1016/j.cej.2012.08.050.
[94] B. Van de Voorde, M. Hezinová, J. Lannoeye, A. Vandekerkhove, B. Marszalek, B. Gil, et al., Adsorptive desulfurization with CPO-27/MOF-74: an experimental and computational investigation, Phys. Chem. Chem. Phys. (2015) 10759–10766, http://dx.doi.org/10.1039/c5cp01063b.
[95] S. Djemel, M.-F. Guilleux, J. Jeanjean, J.F. Tempere, D. Delafosse, Effect of Ce3+ ions exchanged in NiX zeolites on the location and reducibility of Ni2+ ions and on the stabilization of a highly dispersed metallic nickel, J. Chem. Soc. Faraday Trans. 1 Phys. Chem. Condens. Phases 78 (1982) 835, http://dx.doi.org/10.1039/f19827800835.